Electronic Supplementary Material (ESI) for RSC Advances.

Supporting Information

Clickable Poly-L-Lysine for the Formation of Biorecognition Surfaces

*Daniele Di Iorio, Almudena Marti, Sander Koeman and Jurriaan Huskens**

Molecular NanoFabrication group, MESA+ Institute for Nanotechnology, University of Twente, Enschede, The Netherlands

Synthesis of PLL-OEG-Tz and PLL-OEG-DBCO

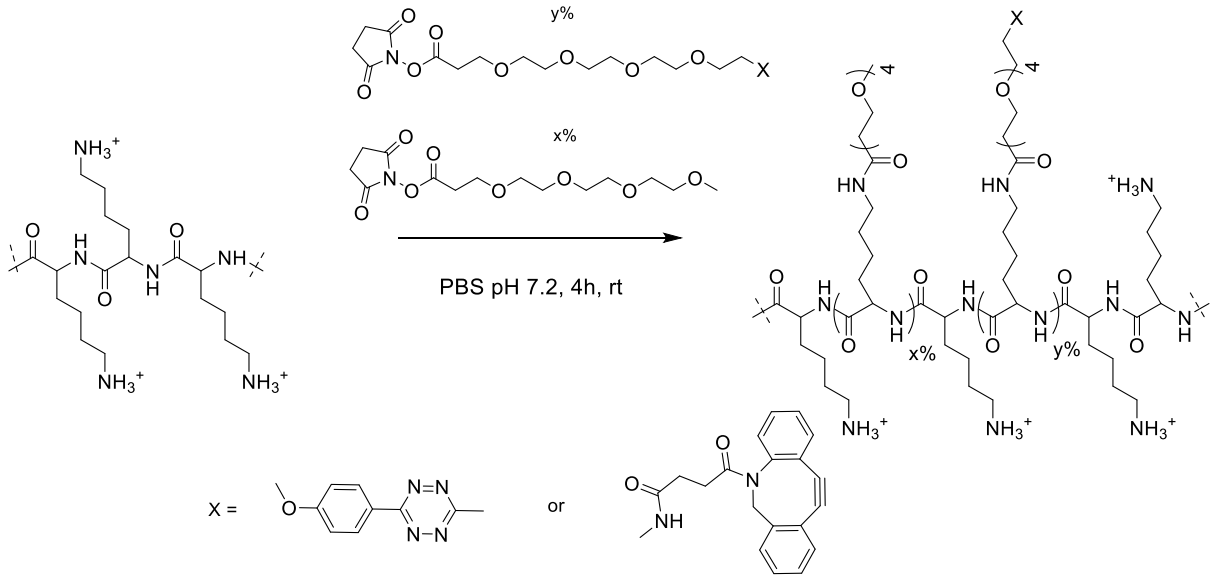

Scheme S1. Synthesis of PLL-OEG-Tz and PLL-OEG-DBCO. PLL is reacted with desired relative ratios of either Tz-OEG_4-NHS or DBCO- OEG_4-NHS, and methyl-OEG_4-NHS ester to give the final modified PLL with the desired degrees of functionalization.

The overall grafting ratio (the percentage of the OEG and OEG-Tz chains) was determined by adapting a previously reported procedure.[1] The grafting densities of tetrazine moieties (y%) were calculated by eqn 1:

$$\%\ functionalization = \frac{\text{integral of one Tz peak}}{\text{integral of free lysine+integral of coupled lysine}} \times 100 \qquad (1)$$

The grafted densities of DBCO moieties (y%) were calculated instead by eqn 2:

$$\%\ of\ functionalization = \frac{(\text{integral of DBCO peak})/4}{\text{integral of free lysine+integral of coupled lysine}}\ x\ 100 \qquad (2)$$

Table S1. Degrees of functionalization of modified PLLs calculated by NMR.

Modified PLL	Free lysine %	Coupled lysine %	Tz/DBCO %
PLL-OEG	72.0	28.0	0
PLL-OEG$_{31.7}$-Tz$_{0.5}$	67.8	32.2	0.5
PLL-OEG$_{26.0}$-Tz$_{4.9}$	69.1	30.9	4.9
PLL-OEG$_{27.3}$-Tz$_{14.6}$	58.1	41.9	14.6
PLL-OEG$_{24.5}$-DBCO$_{6.7}$	68.8	31.2	6.7

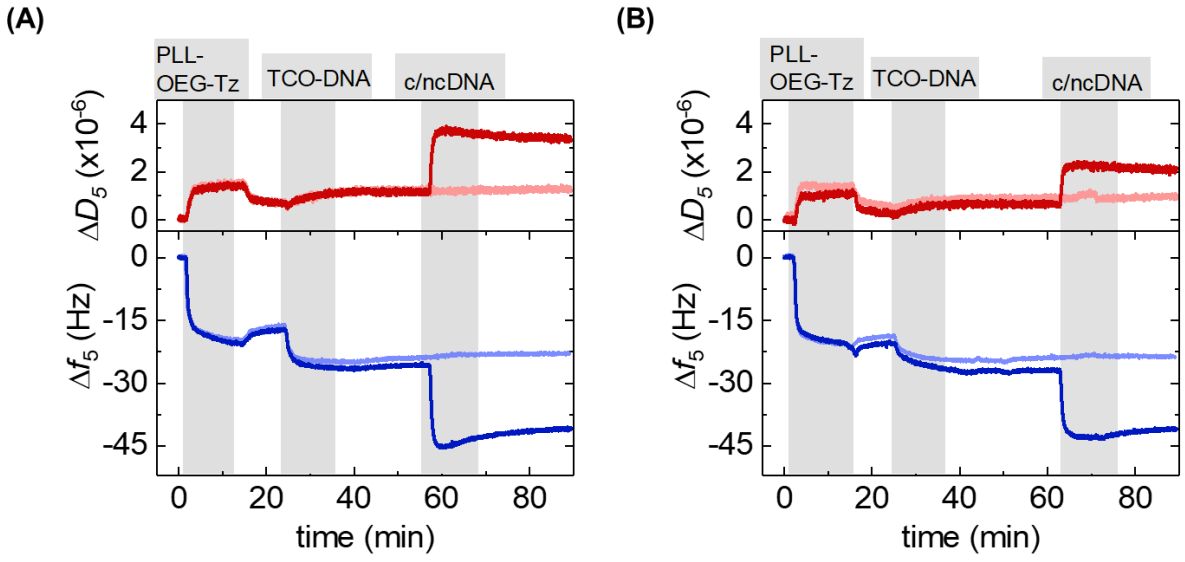

Figure S1. QCM-D sensograms of the assembly of PLL-OEG(26.0)-Tz(4.9) (0.1 mg/mL in PBS) on silicon dioxide (A) and gold (B) surfaces, followed by TCO-DNA (1 µM in PBS) and cDNA (1 µM in PBS). The frequency shift (Δf_5) is represented by the blue lines and the dissipation signal (D_5) by the red lines. The dark-colored lines represent traces using cDNA, while the light-colored ones indicate the use of ncDNA as a control. All adsorption steps are shown in grey vertical bars, while the washing steps with PBS are in white.

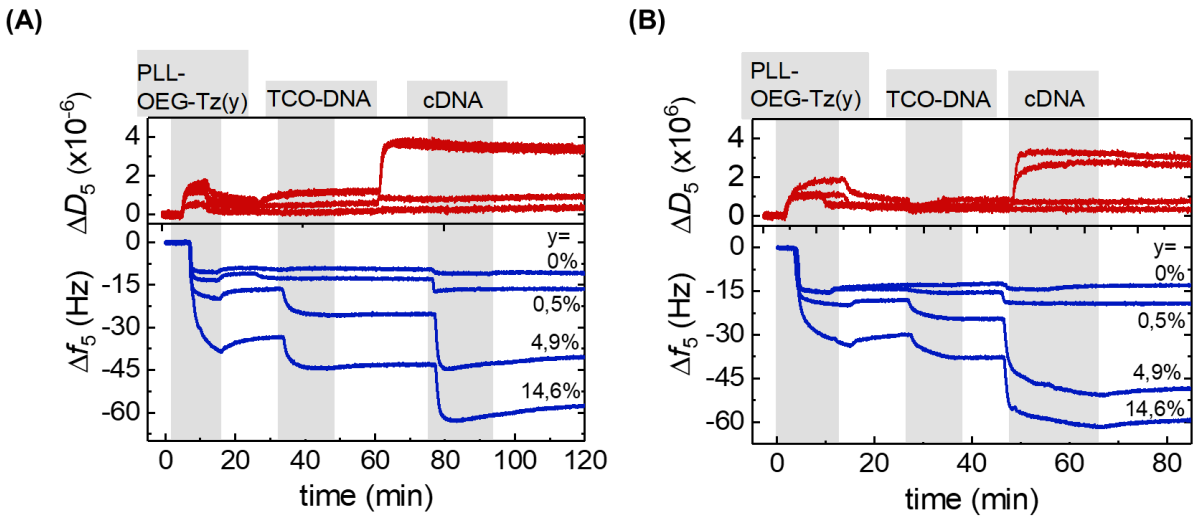

Figure S2. QCM-D sensograms of the assembly of PLL-OEG-Tz functionalized with varying percentages of Tz (y = 0, 0.5, 4.9 and 14.6%), followed by coupling with TCO-DNA and adsorption of cDNA, for both SiO_2 (A) gold (B) substrates. The frequency shift (Δf_5) is represented by the blue lines and the dissipation signal (ΔD_5) by the red lines.

Comparison between SiO_2 and gold substrates

Some differences in the adsorption steps were, however, observed for the two types of substrates. First of all, the TCO-DNA steps appeared to be larger on SiO_2 surfaces compared to gold. Moreover, adsorption of cDNA appeared to be larger on the gold surface indicating a higher hybridization efficiency and/or a difference in the degree of hydration. At the same time, some dissipation changes were observed for the TCO-DNA adsorption steps, whereas smaller increments were observed on gold substrates compared to SiO_2. These observations may suggest that differences in the substrate charge occur after activation which might influence the adsorption of TCO-DNA and cDNA in subsequent steps and/or the hydration of the layer. As a consequence, the apparent hybridization efficiency, defined as the ratio of the frequency shifts induced by cDNA and TCO-DNA, was higher for gold surfaces compared to silicon dioxide. By taking into account the different lengths of the TCO-DNA (15 nts) and cDNA (36 nts), hybridization efficiencies (uncorrected for possible differences and changes in hydration) of 130% and 65% were obtained for gold and silicon dioxide surfaces, respectively. Different DNA lengths as well as the formation of a DNA duplex can cause a change in the degree of hydration, which is detected by QCM.[2, 3]

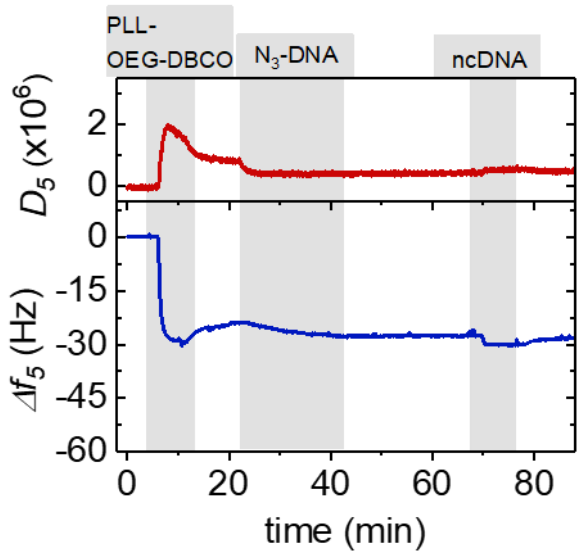

Figure S3. QCM-D sensograms of the assembly of PLL-OEG-DBCO(6.7) (0.1 mg/mL in PBS) on silicon dioxide surfaces, followed by N_3-DNA (1 µM in PBS) and ncDNA (1 µM in PBS). The frequency shift (Δf_5) is represented by the blue line and the dissipation signal (ΔD_5) by the red line. All adsorption steps are shown in grey vertical bars, while the washing steps with PBS are shown in white.

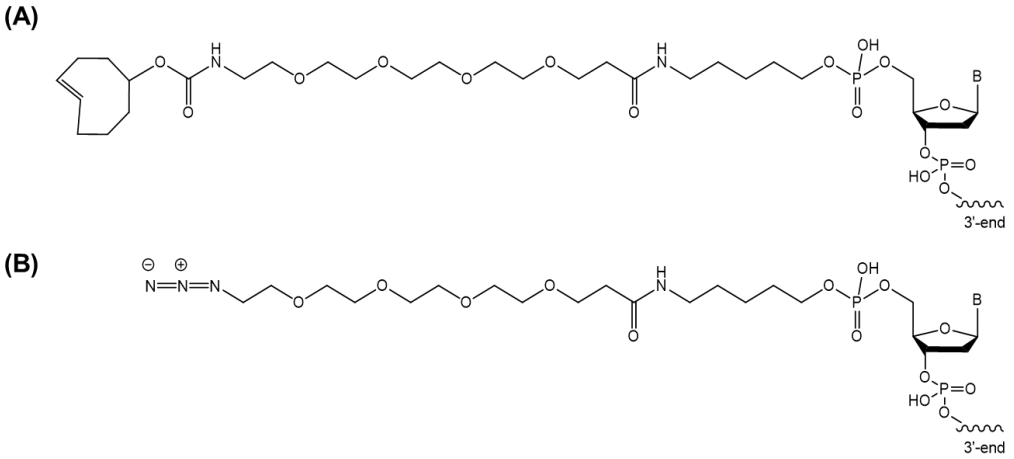

Figure S4. Chemical structures of the TCO linker (A) and of the azido linker (B) used in this work for the modified DNA sequences. The exact sequences are described in the Materials.

Quantification of DNA

The surface coverage of DNA was calculated by using the following equation:

$$Q_{total} = \frac{2nFAD_0{}^{1/2}C_0^+}{\pi^{1/2}} t^{1/2} + Q_{dl} + \mathrm{n}FA\Gamma_0 \qquad (4)$$

Where n is the number of electrons in the electrode reaction (n=1), F is the Faraday constant (96485 C/equivalent), A is the electrode area (0.044 cm^2), Q_{dl} is the capacitive charge (C), $nFA\Gamma_0$ is the charge produced by the adsorbed RuHex and Γ_0 is the amount of RuHex confined on the electrode surface (mol/cm^2). The intercept at t = 0 is the sum of the capacitive charge (Q_{dl}) and the surface excess terms ($nFA\Gamma_0$).

$$Q_{\mathrm{total}}=Q_{\mathrm{dl}}+\mathrm{n}FA\Gamma_0 \qquad (5)$$

To achieve a much more indicative view of DNA surface density, a meaningful conversion is necessary. Γ_{DNA}, the probe coverage in molecules/cm^2, can be written as in Eq. 5, where m is the number of base pairs in the DNA, z is the charge of the redox molecules (z=3) and N_{A} is Avogadro's number.

$$\Gamma_{DNA} = \Gamma_0 \left(\frac{z}{m}\right) N_A \qquad (6)$$

Substituting Eq. 5 into Eq. 6:

$$\Gamma_{DNA} = \frac{Q_{total} - Q_{dl}}{nFA}\left(\frac{z}{m}\right)N_A \qquad (7)$$

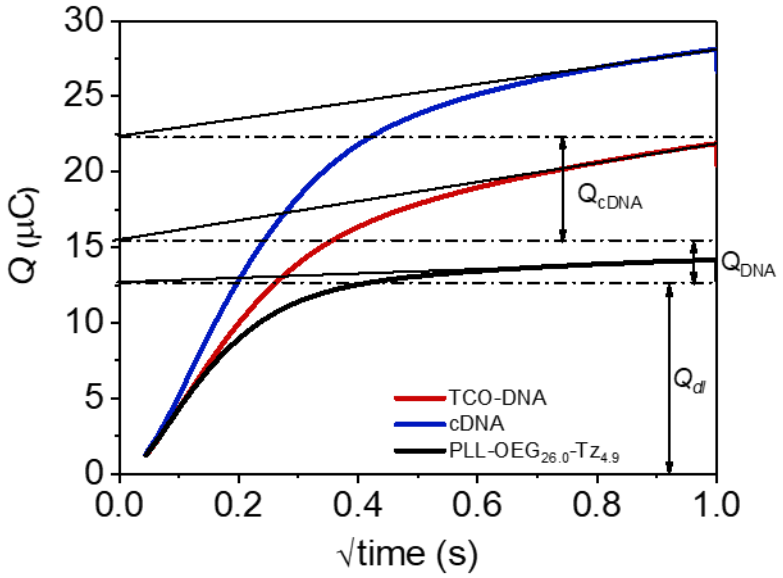

Figure S5. CC measurements showing a typical DNA density calculation. The represented Figure is the same as Figure 3.5, with additional indications for the calculation of DNA densities, where Q_{dl} represents the capacitive charge, Q_{DNA} is the measured charge for TCO-DNA and Q_{cDNA} is the charge measured upon addition of cDNA.

Supporting References

1. J. Movilli, A. Rozzi, R. Ricciardi, R. Corradini and J. Huskens, *Bioconjugate Chemistry*, 2018, **29**, 4110-4118.
2. C. Larsson, M. Rodahl and F. Höök, *Analytical Chemistry*, 2003, **75**, 5080-5087.
3. X. Su, Y.-J. Wu and W. Knoll, *Biosensors and Bioelectronics*, 2005, **21**, 719-726.